MINISTRY OF EDUCATION
AND TRAINING

VIETNAM ACADEMY
OF SCIENCE AND TECHNOLOGY

GRADUATE UNIVERSITY OF SCIENCE AND TECHNOLOGY

PHẠM ĐỒNG BẰNG

RESEARCH AND DEVELOPMENT OF LARGE APERTURE LIDAR TECHNIQUE FOR STUDYING UPPER ATMOSPHERE PARAMETERS

Specialization: Optics
Numerical code: 9 44 01 10

SUMMARY OF DOCTORAL THESIS IN MATERIAL SCIENCE

HANOI, 2025

The thesis was completed at:
Department of Physics, Graduate University of Science and Technology, VAST
Center of Engineering Physics, Institute of Physics, VAST

Supervisors: **Assoc. Prof. Dr. Dinh Van Trung**
Assoc. Prof. Dr. Pham Hong Minh

Reviewer1:
.....

.....

Reviewer2:
.....

.....

Reviewer3:
.....

.....

The thesis will be defended at:
.....
.....
Time:.....

The thesis could be found at:
- National Library of Vietnam
- Library of Graduate University Science and Technology
- Library of Institute of Physics

PREFACE

In recent decades, the issue of global climate change has become one of the greatest challenges facing humanity, attracting special attention from scientists and governments around the world [3, 4].

Based on the recognition of the importance and necessity of developing large-aperture lidar technology, I chose the topic "Research on the development of large-aperture lidar technology for studying upper atmospheric parameters" as my doctoral research topic.

The thesis is structured into 3 chapters:

Chapter 1: Overview of the upper atmosphere and lidar techniques

Chapter 1 presents an overview of the structure and stratification of the Earth's atmosphere and some characteristics of the upper atmosphere, the influence of atmospheric parameters on the weather and environment on Earth. The theoretical basis of the interaction of light with molecules in the atmosphere is based on Rayleigh elastic scattering and Mie scattering.

Chapter 2: Research and development of large aperture lidar systems

Chapter 2 presents the structure and operating principles of the lidar system in general. Design and development of the lidar system with a large aperture spherical mirror. The development of the optical receiver with a spherical mirror with a diameter of 60 cm includes the mirror manufacturing process and the measurement of the mirror surface profile. To evaluate the signal quality of the lidar system that has been upgraded with a large aperture, we conducted simulations and experimental measurements to compare the results.

Chapter 3: Characteristics of upper atmosphere parameters

The final chapter of the thesis presents the results of the survey of the upper atmosphere. The results of the survey of the cirrus cloud

determined the height of the cloud top, bottom, physical characteristics such as temperature, optical depth and lidar ratio. This part of the results was performed on a lidar system with a Schmidt-Cassegrain optical receiver.

The next part of the results is the survey of the temperature parameters of the upper atmosphere, performed on a lidar system with an upgraded receiver using a large aperture spherical mirror, with a diameter of 60 cm, which has been manufactured. The results of the received signal measurements are very consistent with the simulated signal path of MSISE-90, showing that the lidar system works well and the results are reliable. From the received elastic lidar signals, we determined the temperature distribution using the temperature distribution determination algorithm. Our temperature distribution curves are compared and evaluated for errors with radiosonde measurements and MSISE-90 simulations, and the results show that they have similar temperature profile.

CHAPTER 1 OVERVIEW OF THE HIGH-LEVEL ATMOSPHERE AND LIDAR TECHNIQUES

1.1 Overview of the Earth's atmosphere

1.1.1. General characteristics of the Earth's atmosphere

The atmosphere is the gaseous shell surrounding the Earth, existing as a mixture of gas and water vapor, covering the entire surface of the Earth with a thickness of up to several hundred kilometers.

1.1.2. Distribution of atmospheric density and temperature

The atmosphere has no clear upper boundary but gradually transitions into space. The distribution of atmospheric density and temperature in each atmospheric layer is uneven and depends on many

factors such as absorption of solar radiation, convective motion, gas composition and the effect of gravity.

1.1.3. High-level clouds

High clouds is a meteorological term used to refer to clouds that appear and exist mainly at high altitudes in the atmosphere, usually from about 6 km to 12 km in temperate and tropical climates and may be lower in polar regions due to atmospheric characteristics at these latitudes.

1.1.4. Atmospheric survey techniques

In atmospheric research, there are many survey methods and techniques used to collect information on the physical, chemical and optical parameters of the atmosphere. The two main groups of methods commonly used are direct observation methods and remote sensing methods.

1.2. Lidar techniques

1.2.1. Interaction of light with the atmosphere

Light as it passes through the atmosphere undergoes various interactions with atmospheric components such as water vapor, gas molecules, aerosols, and clouds. These interactions result in a decrease in the energy of light as it travels from outer space to the Earth's surface, mainly through two important processes: scattering and absorption.

1.2.2. Rayleigh scattering

Rayleigh scattering is a phenomenon of light scattering that occurs when electromagnetic waves (light) interact with gas molecules that are very small in size, much smaller than the wavelength of the incident light (usually the size of the molecule is about 1/10 smaller than the wavelength).

1.2.3. Mie scattering

As the size of the aerosol approaches the wavelength of the incident radiation, the scattering phenomenon changes greatly. The Mie scattering theory is used to describe the scattering of aerosols in this case.

1.2.4. Theoretical basis for determining temperature distribution

Atmospheric temperature can be calculated from the molecular properties of the atmosphere based on the assumption of hydrostatic equilibrium and the ideal gas law by integrating the hydrostatic equation with respect to altitude.

$$T(z_{i+1}) = \frac{\rho(z_i)}{\rho(z_{i+1})} T(z_i) + \frac{mg\left(\frac{z_i+z_{i+1}}{2}\right)}{R} \Delta z \frac{\rho(z_i) - \rho(z_{i+1})}{\ln\left(\frac{\rho(z_i)}{\rho(z_{i+1})}\right)} \quad (1)$$

1.2.5. Long-distance measurement

Lidar technique is a modern and effective method in remote atmospheric research [64]. However, lidar also has certain limitations when measuring large distances, especially when surveying the upper layers of the atmosphere.

1.3. Application of lidar technique in atmospheric research.

1.3.1. In the world

Around the world, many countries such as the United States, Japan, Germany and India have invested heavily in upper atmospheric research, mainly in mid- and high-latitude regions.

1.3.2. In Vietnam

In Hanoi in particular and Vietnam in general, research related to the upper atmosphere is mainly carried out within the framework of scientific projects of research institutes and specialized universities.

1.4 Conclusion of Chapter 1

Chapter 1 presents an overview of the structure and characteristics of the Earth's atmosphere, especially the upper

atmosphere, and its important role in global meteorological and climate processes. The specific contents presented include:

- Basic characteristics of the Earth's atmosphere, including stratified structure, main chemical composition and changes in atmospheric density and temperature with altitude.
- Characteristics, classification and formation mechanism of high-level clouds, as well as their role in radiation balance, water cycle and global climate change.
- Popular atmospheric survey techniques, including direct measurement methods such as weather balloons and meteorological rockets, and modern remote sensing methods such as radar, satellites and lidar.
- Theoretical basis and mathematical models of light scattering processes in the atmosphere (Rayleigh and Mie), which are important foundations for applications in lidar techniques.
- The limitations and practical applications of lidar techniques in measuring atmospheric parameters, especially in the upper atmosphere, emphasize the importance and necessity of developing modern lidar systems with large apertures. Through the presented contents, Chapter 1 clearly affirmed the key role of modern survey methods, especially lidar, in providing important data for further research on the upper atmosphere, supporting climate studies, improving the accuracy and reliability of weather and climate forecasting models. This is the theoretical and practical basis for developing large aperture lidar techniques to improve the ability to measure and survey the upper atmosphere more comprehensively and effectively.

CHAPTER 2 RESEARCH AND DEVELOPMENT OF LARGE APERTURE LIDAR SYSTEM

2.1. Lidar measurement system

2.1.1. Basic structure of lidar measurement system

A typical atmospheric lidar system consists of two main components: a transmitter and a receiver, along with associated signal processing and control components.

2.1.2. Elastic lidar system configuration using Schmidt-Cassegrain telescope

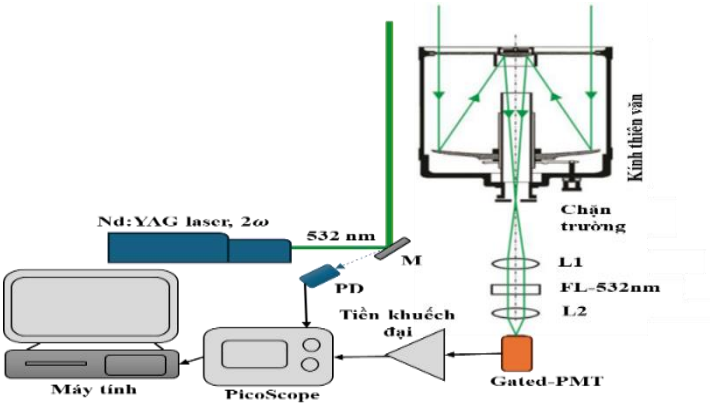

Figure 2.1. Configuration of a single-channel elastic lidar system using a Schmidt-Cassegrain telescope developed at the Institute of Physics .

The figure shows the detailed configuration of an elastic lidar system with a Schmidt-Cassegrain telescope receiver of 25.4 cm diameter and 2.5 m focal length to survey high-level cirrus clouds.

2.1.3. Elastic lidar system configuration using large aperture spherical mirror

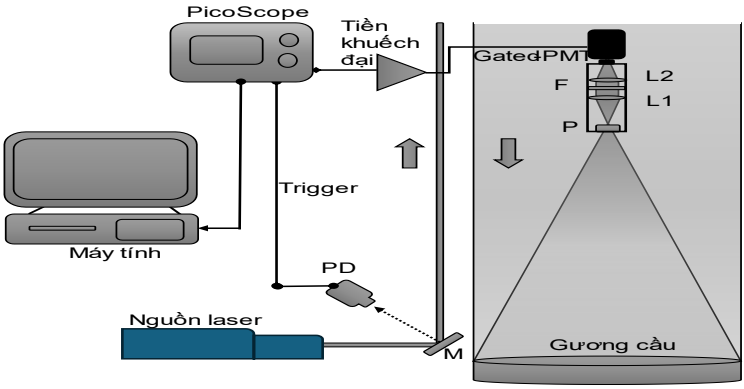

Figure 2.2. Configuration of a single-channel elastic lidar system using a large-aperture spherical mirror.

Based on the elastic lidar system configuration using Schmidt-Cassegrain telescope. We proceed to build the configuration of the large aperture elastic lidar system. The upgraded elastic lidar system is developed for the purpose of atmospheric survey at large distances, with the system configuration diagram shown in Figure 2.2.

2. 2 Characteristic parameters of parts and components in the large aperture lidar system

2.2.1. Laser source

The transmitter block of the large-aperture lidar system uses a pulsed Nd:YAG laser source (Brilliant model, Quantel, France) with a fundamental wavelength of 1064 nm [70]. This is a type of laser capable of emitting high-power and stable pulses.

2.2.2. Optical signal receiver and filter

The receiver of the large aperture lidar system uses a spherical mirror researched and manufactured by the team. Choosing the size and focal length of the spherical mirror is an important factor in upgrading the receiver for the lidar system.

2.2.3. Photomultiplier tube

Photon Multiplier Tube (PMT) is a highly sensitive optoelectronic device used to detect weak light and convert it into an electrical signal. When a photon strikes the optical window of the PMT, it passes through and interacts with the photocathode layer, generating photoelectrons through the photoelectric effect.

2.2.4. Signal processor

The electrical signal from the photomultiplier tube is amplified before being sent to the analog-to-digital converter. The amplifier module has low signal distortion and a maximum bandwidth of up to 1.2 GHz, and the amplifier gain is 20 times.

2.3. Process of manufacturing spherical mirrors

2.3.1. Theoretical basis for calculating and selecting spherical mirror size parameters

To design and build an effective atmospheric survey lidar system, determining the optimal parameters, especially the receiver mirror diameter, plays an important role.

2.3.1.1. Theoretical model

Rayleigh lidar signal equation:

$$P(z) = \frac{E_0 \cdot \frac{c}{2} \cdot \eta \cdot A_r \cdot \beta_R(z).T^2(z)}{z^2}, \qquad (2.2)$$

2.3.1.2. Simulation results of selecting spherical mirror parameters

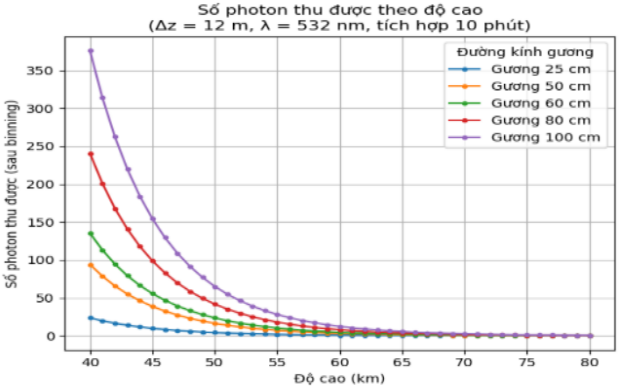

Figure 2.3. Representation of the number of photons collected by the lidar system at different heights when using a spherical mirror optical receiver with a diameter from 25 to 100 cm.

The graph shows the number of photons collected at altitude (40–70 km), with different mirror diameters (25, 50, 60, 80 and 100 cm), spatial resolution of 12 m, integration time of 10 min.

2.3.2. Manufacturing a spherical mirror

The goal is to manufacture a spherical mirror with a diameter of 60 cm and a focal length of 1.8 m. For this parameter, the mirror blank needs to meet the thickness and hardness. Because the selected glass blank is only 19 mm thick, not enough to ensure these criteria, the research team applied the baking technique to join the glass plates, creating a thicker mirror blank, ensuring stability.

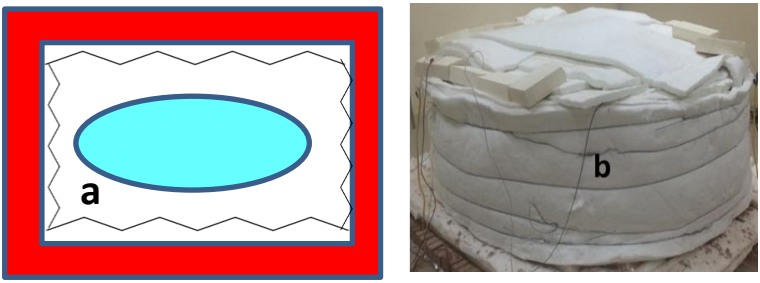

Figure 2.4. Electric furnace: a) Furnace model; b) Actual furnace.

2.3.3. Evaluation of the surface profile of spherical mirrors

The Foucault method is an important technique for measuring the profile of spherical and aspherical mirrors with large apertures without the need for a reference surface. Compared with traditional measurement methods, this method has the advantages of high accuracy and fast execution time [76].

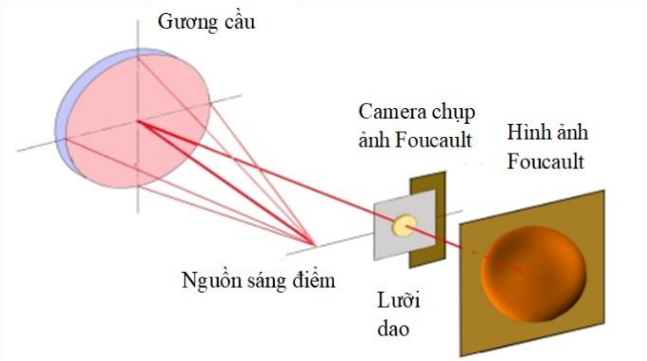

Figure 2.5. Schematic diagram of the Foucault method for testing the surface of a spherical mirror [76].

Hartmann method

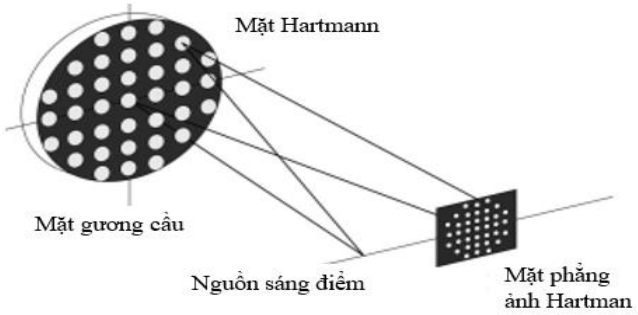

Figure 2.6. Hartmann principle diagram [76].

The Hartmann method is used to check the profile of optical mirrors by splitting an incident light beam into many small rays through a perforated mask. When the light rays are reflected from the mirror surface, their deviation helps determine the deformation of the mirror surface from the ideal.

The reflectivity of an aluminum-plated spherical mirror depends on the wavelength of the light it reflects [77]. An aluminum-plated spherical mirror has good reflectivity, especially in the visible light region, part of the ultraviolet (UV) region and the infrared (IR) region. The reflectivity of aluminum in the visible light region with wavelengths from 400 nm to 700 nm typically ranges from 85% to 90%.

Figure 2.7. 60 cm diameter spherical mirror after aluminum plating.

2.4. Evaluation of large aperture lidar system

2.4.1. Installation of large aperture lidar system

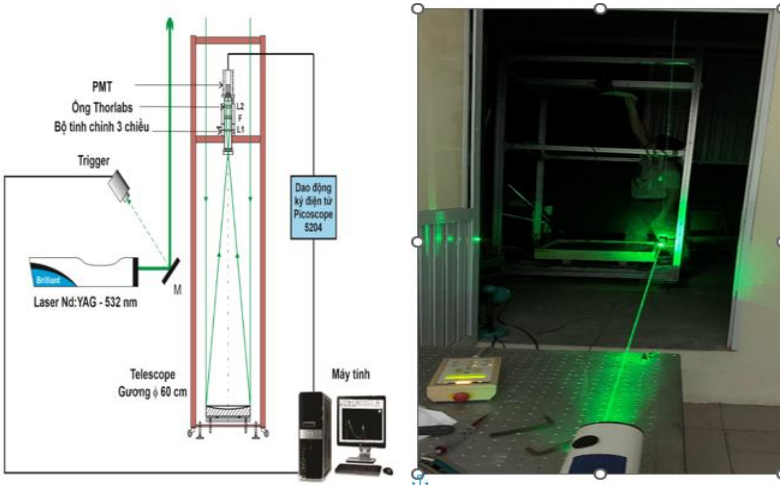

Figure 2.8. Design diagram and actual lidar system with 60 cm diameter spherical mirror.

2.4.2. Simulation of lidar signal reception

Calculations and simulations were performed with the parameters of the designed system with a mirror diameter of 60 cm and a focal length of 1.8 m. The simulation results in Figure 2.9 show that in both cases, the overlap function has almost the same characteristics: starting at 0 at low altitudes, then gradually increasing to 1 at altitudes above 800 m.

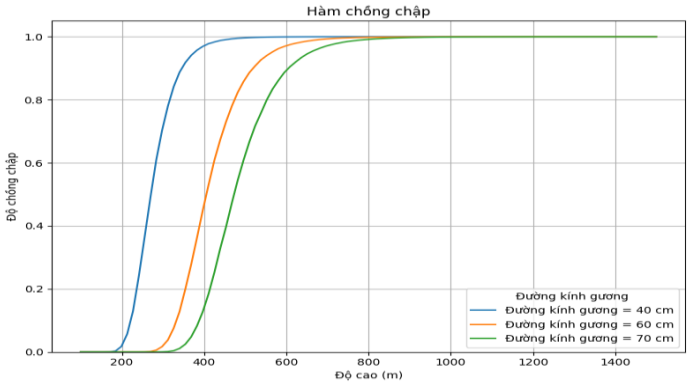

Figure 2.9. Overlap function.

The simulation results of the light intensity images obtained at the focal plane are shown in Figure 2.10a and Figure 2.10b. The reflected images obtained have a shape similar to a triangle in both the spherical and parabolic mirror cases. However, the light intensity is concentrated at the edge for the spherical mirror and distributed more evenly in the parabolic mirror case, this feature may be due to the reflective properties of the mirror surface.

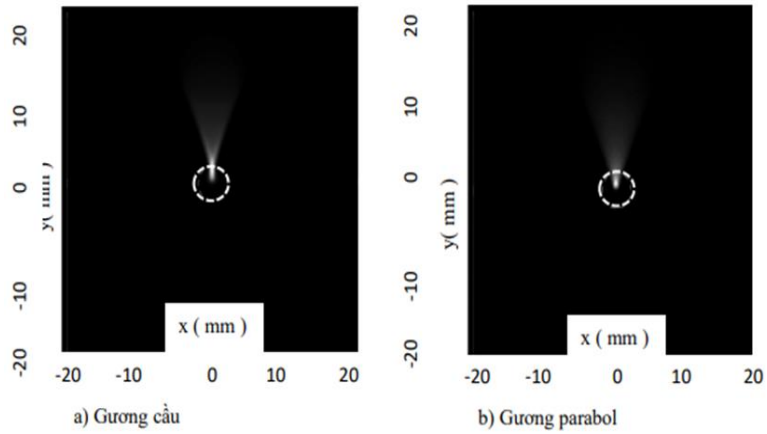

Figure 2.10. Simulation results of images obtained at the focal plane and above of a) spherical mirror and b) parabolic mirror, the circle represents the pinhole blocking the field.

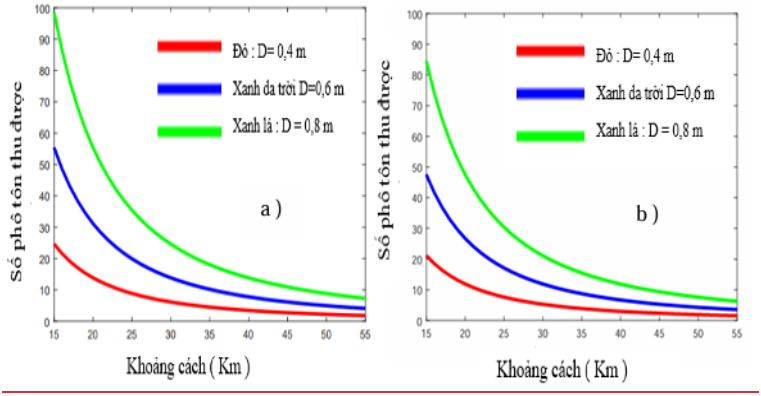

Figure 2.11. Numerical simulation of backscattered elastic photons collected at the photoelectric receiver system a) Transfer function T = 0.96 b) Transfer function T = 0.93.

The figure simulates the number of photons collected according to the distance from the scattering center to the lidar receiver system. The number of photons collected is proportional to the area of the optical lens which is a spherical mirror. We simulate and calculate the number of photons collected with optical lenses with diameters of 0.4 m; 0.6 m; 0.8 m respectively.

2.4.3. Comparison of simulation results and lidar signals at the focal plane of the lidar receiver system

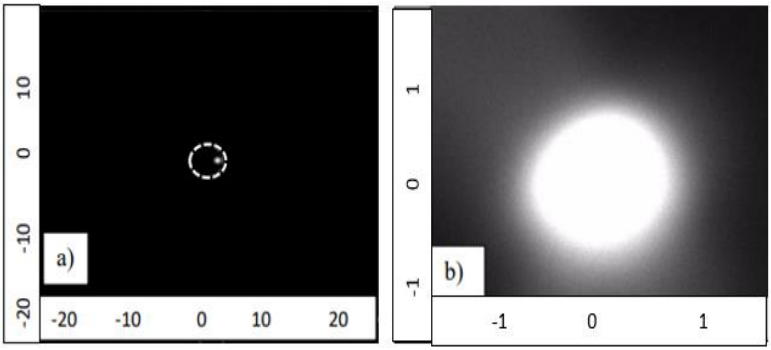

Figure 2.12. Laser cross-section image collected at a plane away from the focal plane.

2.5. Conclusion of chapter 2

Chapter 2 presented the research and development process of a lidar system using a large-aperture optical receiver to improve signal reception. The system was built on the basis of a single-channel elastic lidar, then upgraded by replacing the Schmidt-Cassegrain telescope with a concave mirror with a diameter of 60 cm and a focal length of 1.8 m. The manufacture of a domestic spherical mirror with a high-reflectivity aluminum coating is an important improvement to improve signal reception capacity.

Based on the modeling of geometry and field of view, factors affecting the reception efficiency such as pulse width, response time, and field of view were investigated in detail. Simulation of the overlap distribution between the transmitting beam and the receiving field area was performed to optimize the system configuration. The simulation results showed that the effective overlap area could be extended from 40 km to over 70 km, thanks to the appropriate design of the spherical mirror, aperture, and detector. Origin, ZEMAX software and simulation tools have been integrated to process the received signals and optimize the system structure.

The thesis also presents in detail the process of measuring the surface of the spherical mirror after fabrication, using the Foucault and Hartmann methods to evaluate the geometric accuracy. The experimental measurement results show that the profile error is less than 0.5 μm and the reflection quality meets the technical requirements for the lidar system. In addition, the thesis simulated the signal response with many environmental and equipment parameters, contributing to determining the relationship between optical design and the ability to detect weak signals at high altitudes.

The results achieved in chapter 2 are an important foundation for the implementation of a complete fabrication of a large-aperture elastic lidar system, serving the observation of atmospheric temperature and surveying of high-level clouds. This is also a testament to the ability to master the design and manufacture of precision optical equipment

domestically, with potential for practical and expanded applications in the fields of meteorology, environment and atmospheric science.

CHAPTER 3 CHARACTERISTICS OF HIGH-LEVEL ATMOSPHERIC PARAMETERS

3.1. Survey of cirrus clouds in Hanoi

3.1.1. Physical basis for determining cirrus cloud parameters

The basic Lidar equation gives us the relationship between the backscattered signal intensity depending on the height z [11, 79]:

$$P(z) = P_{laser}.C.Z^{-2}.[\beta_c(z) + \beta_m(z)].T_c^2(z).T_m^2(z)\,. \qquad (3.1)$$

3.1.2. Cirrus Cloud Height

Due to the high ice crystal content, cirrus clouds have the ability to strongly scatter laser light, creating high intensity backscatter signals in lidar observations.

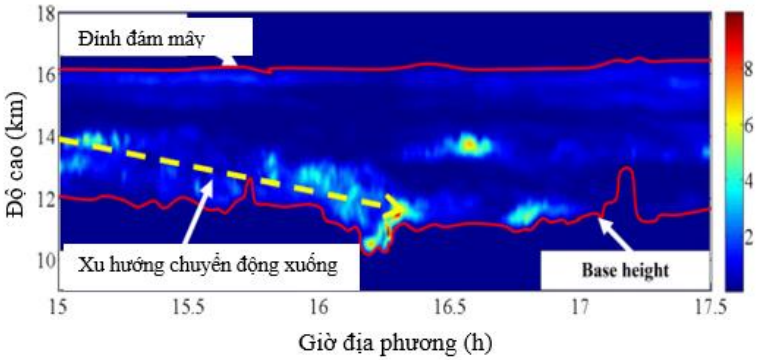

Figure 3.1. Cirrus cloud observation, the color-coded intensity represents the distance-corrected lidar signal intensity.

3.1.3. Geometric thickness and optical depth of cirrus clouds

Studying this relationship helps improve the assessment of the radiative impact of high-level clouds and contributes to climate models in simulating global climate change [58].

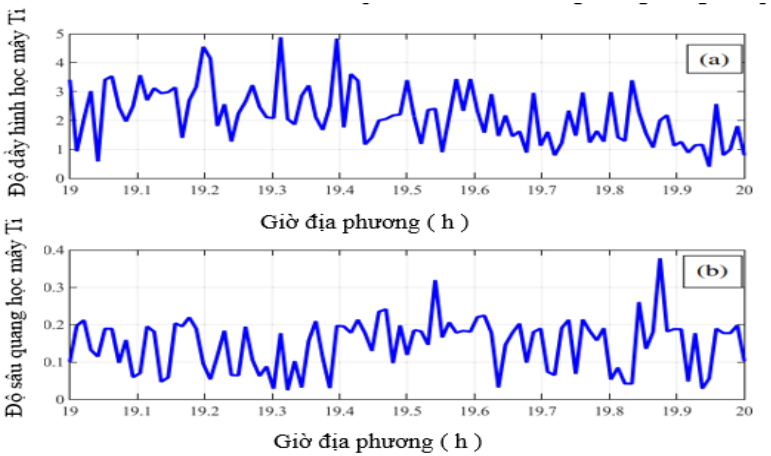

Figure 3.2. (a) Real-time variation of the geometric thickness of cirrus clouds (b) temporal variation of the optical depth of cirrus clouds obtained from the same data.

3.1.4. Lidar ratio of cirrus clouds

Based on the obtained lidar data, we determined the lidar ratio for several Ti cloud cases. The average value of the measured lidar ratio was 30 ± 18, which is within a relatively large range of variation, reflecting significant differences between the observed clouds.

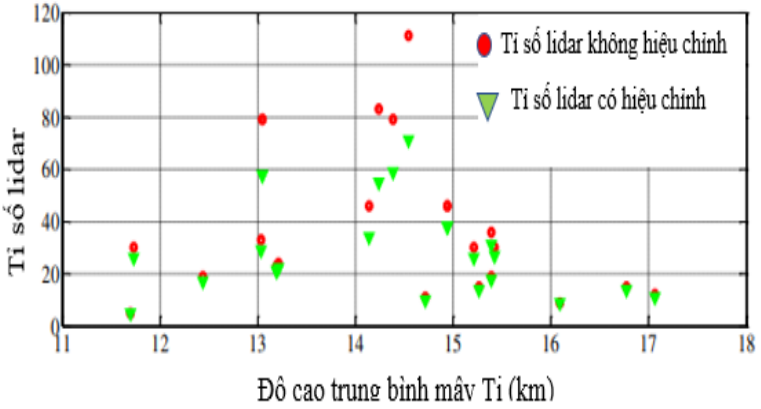

Figure 3.3. Lidar ratio without correction and correction for the average cloud height of cirrus clouds.

3.1.5. Results of survey of cirrus cloud temperature parameters.

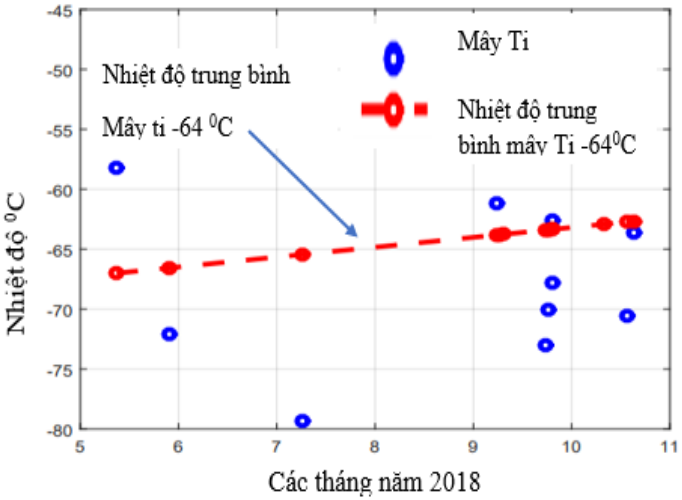

Figure 3.4 shows the results of the cirrus cloud temperature survey during the period from May to November 2018.

3.1.6. Statistics of cirrus cloud lidar measurements

Such quantitative statistics do not only provide an overall view of the frequency of cirrus cloud occurrence..

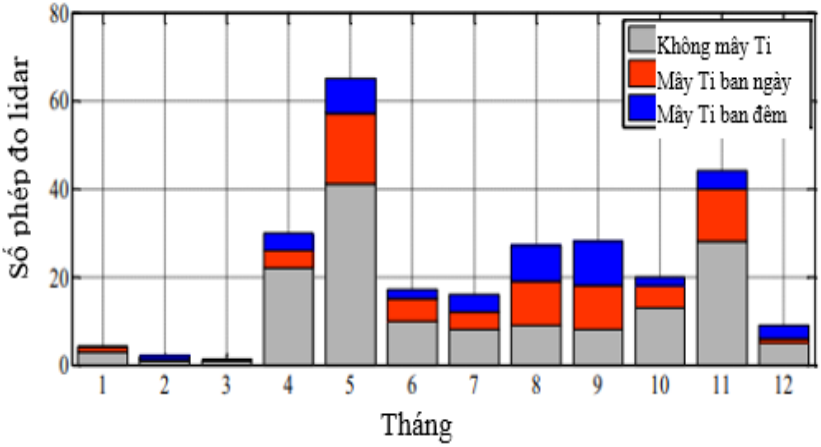

Figure 3.5. Statistical chart of the number of occurrences of cirrus layers and the total number of lidar measurements from 2011 to 2017.

3.2. Determination of physical parameters of the upper atmosphere

3.2.1. Algorithm for determining temperature distribution

With the signals meeting the requirements, we smooth the signal over time and space by averaging 20 points on a logarithmic scale.

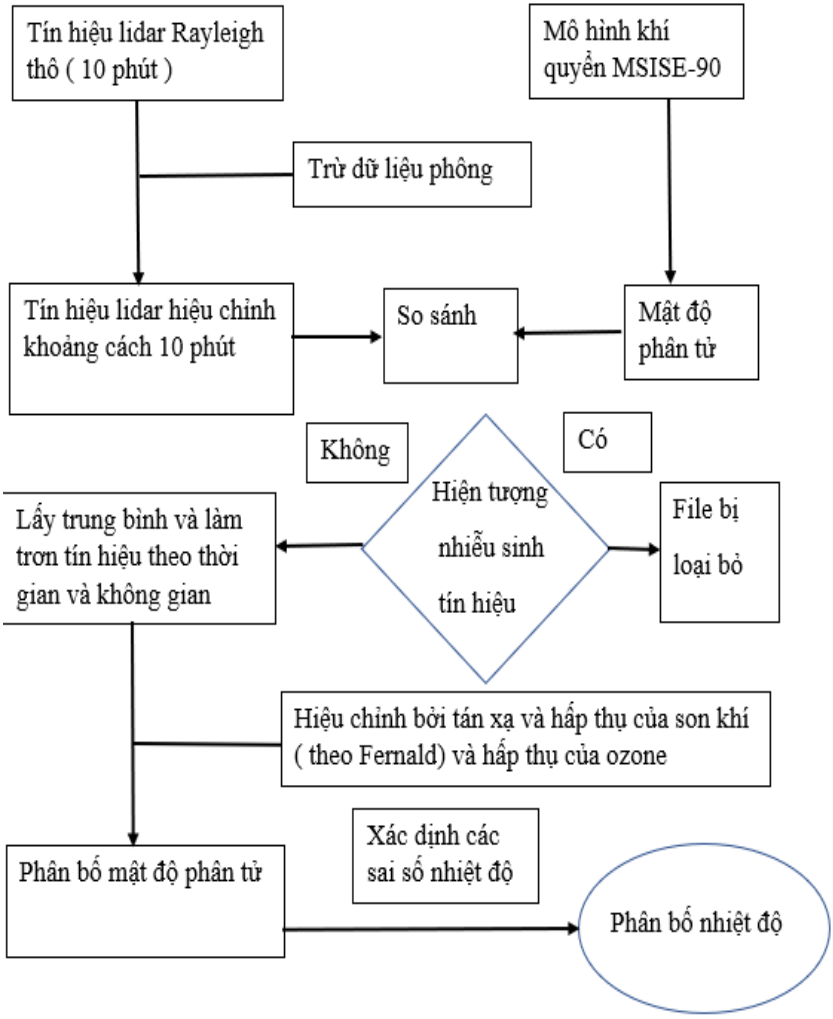

Figure 3.6. Block diagram of the temperature algorithm.

3.2.2. Evaluation of lidar signal quality obtained from aperture mirror lidar system

The obtained signals demonstrated that the current lidar system can provide stable and accurate signals up to an altitude of about 40–45 km.

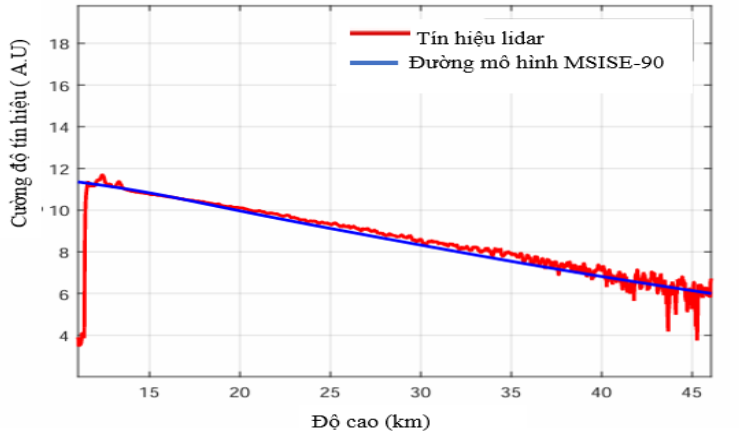

Figure 3.7. Lidar signal at 10:00 p.m. on August 25, 2018 at 18 Hoang Quoc Viet- Nghia Do- Cau Giay- Hanoi.

3.2.3. Determination of molecular density from effective lidar signal

The effective lidar signal is obtained by dividing the measured lidar signal by the ozone transmission coefficient.

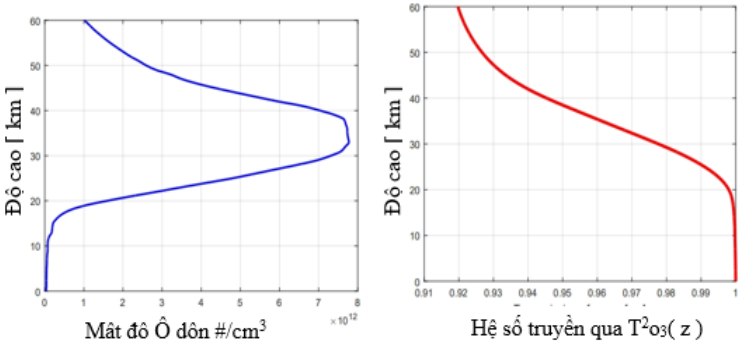

Figure 3.8. Ozone density and ozone transmission with a round trip path to and from the lidar receiver.

3.2.4. Errors in determining atmospheric temperature from lidar measurements

Temperature errors in integrated lidar temperature measurements can originate from various sources such as: aerosol errors, ozone absorption, statistical noise, selected reference temperature, cloud absorption.

3.2.5. Temperature distribution and temperature error of lidar measurements for upper atmosphere surveys.

Using the algorithm as described to calculate the temperature gives the result shown in Figure 3.9.

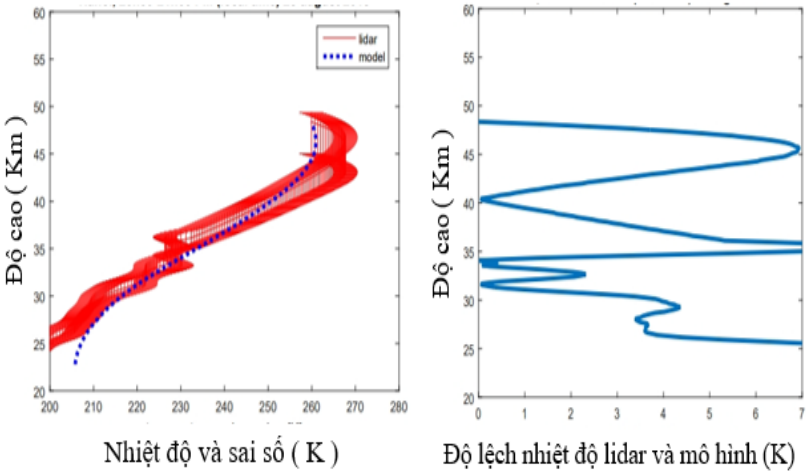

Figure 3.9. Errors and temperature deviations compared to the model.

3.3. Conclusion of chapter 3

The first part is the survey results of cirrus clouds using a lidar system using a Schmidt-Cassegrain optical lens with a diameter of 25 cm and a focal length of 2.5 m. The research results of the group were obtained when surveying cirrus clouds, the height of cirrus clouds in Hanoi is mainly distributed from 6.7 km to 18.0 km with an average height of 14.0 km. The geometric thickness of cirrus clouds ranges from 0.2 km to 7 km, with an average value of 2.3 ± 1.2 km. Our results show that cirrus clouds appear in Vietnam with a thickness almost similar to other studies in the world but in a larger range of altitude. Our research

group also obtained an average optical depth of cirrus clouds of 0.32 ± 0.22 and an average lidar ratio of 30 ± 18 for cirrus clouds detected during the measurement period.

The final part is the survey results using the lidar system upgraded with a large aperture spherical mirror optical receiver. The measurements have obtained elastic signals from the upper atmosphere, the signal path reaches an altitude of over 50 km. The obtained lidar signal path is consistent with the MSISE-90 simulation path. With the measured data, we have determined the atmospheric temperature distribution up to an altitude of 60 km. Our results are consistent with other studies in the world and also consistent with the MSISE-90 atmospheric model.

CONCLUSION OF THE THESIS

The thesis has focused on comprehensive and systematic research on the design, development and application of a lidar system using a large-aperture optical receiver to survey the upper atmosphere in the Hanoi area. This research not only contributes to clarifying the structure and characteristics of the atmosphere in Vietnam, but also demonstrates a significant step forward in mastering modern observation technology using lidar - an advanced technology that is widely used in the fields of meteorology, climate and environment. In terms of theory, the thesis has presented a solid scientific basis for the entire research process.

Basic physical phenomena such as Rayleigh scattering and Mie scattering have been presented and analyzed fully, focusing on the interaction mechanism of laser light with atmospheric components such as gas molecules, aerosols and clouds, especially high-level clouds. Based on standard lidar theoretical models, inverse equations have been developed and calibrated using modern signal processing techniques, allowing accurate retrieval of atmospheric physical parameters. The feedback correction method for lidar signals has also been effectively

applied to eliminate the effects of aerosols and ozone, thereby improving the reliability of determining the attenuation coefficient, backscattering coefficient and gas molecular density.

In terms of technology, a prominent contribution of the thesis is the successful design, manufacture and calibration of an optical receiver using a spherical mirror with a diameter of 60 cm - marking a new step in the capacity of researching and manufacturing optical equipment in the country. The mirror manufacturing process is carried out with high precision through many complex stages, from rough grinding to super-fine polishing, using specialized materials and equipment. The results of optical measurement methods show that the mirror surface has a deviation of less than 0.5 μm and the focal length meets the design requirements, fully meeting the strict technical standards in lidar applications.

The thesis also developed a simulation model of lidar signal transmission in the atmosphere based on Ray-tracing techniques, allowing detailed analysis of the signal attenuation process and the influence of real atmospheric factors such as aerosol density, cloud layer or gas layer fluctuations. This model not only supports the evaluation of system performance but is also an effective tool to optimize the measurement time and the maximum observable height.

Experimental measurement campaigns conducted in Hanoi have confirmed the effectiveness and stability of the developed lidar system. The system allows for clear signal acquisition up to an altitude of 55–60 km with a short measurement time, reflecting superior capabilities compared to previous systems. Based on the measured data, the thesis analyzed the physical characteristics of high-level clouds such as base height, top height, geometric thickness, optical depth and lidar ratio. The obtained values are consistent with the characteristics of cirrus clouds in the tropics and show high compatibility when compared with studies in the world.

In addition, the Rayleigh signal is used to retrieve the temperature distribution of the upper atmosphere. The results show good

compatibility between the temperature measured from the lidar and the standard atmospheric model in the altitude range from 25 to 45 km, with the deviation not exceeding ±7 K. In particular, the thesis determined the location of the stratospheric stratum in the Hanoi area, confirming the reliability of the system and the data processing process.

Overall, the thesis has completed all the research objectives set out. The main contributions include:

- Developing the lidar system using the first large-aperture optical receiver in Vietnam.
- Successfully fabricated a 60 cm diameter spherical mirror with high quality.
- Developed a comprehensive lidar signal processing and calibration process, from modeling to atmospheric influence correction.
- Measured and analyzed the characteristic parameters of high-level clouds and mid-to-upper atmosphere temperature.
- Evaluated the reliability of the lidar system through comparison with standard atmospheric models and international results.

The results of the thesis not only have scientific value but also have the potential for wide practical application, contributing to the construction of an automatic atmospheric monitoring system, serving weather forecasting, climate research and assessing the impact of climate change in Vietnam.

LIST OF PUBLISHED SCIENTIFIC WORKS

1. Hai V. Bui, Manh D. Le, Trung V. Dinh, Tuan X. Nguyen, Tien M. Pham, Hung N. Tran, Bang D. Pham, Bao T. T. Nguyen, Binh T. Nguyen, Hung D. Nguyen, *Optical and geometrical properties of cirrus clouds from lidar measurements above Hanoi*, Vietnam, J. Appl. Remote Sens. 13(3), 034523 (2019).

2. Dinh-V-Trung, Bui Van Hai, Nguyen Thi Thanh Bao, Pham Dong Bang, Vu Thi Kim Oanh, Nguyen Xuan Tu, Phung Viet Tiep, Pham Hong Minh and Nguyen Gia Cuong, *Development of Multi-axis Differential Optical Absorption Spectroscopy System and its application in measuring atmospheric NO2 volume mixing ratio in Hanoi*, Communications in Physics, Vol. 32, No.4 (2022).

3. Bui Van Hai. Nguyen Thanh Hai. Dang Hai Ninh. Pham Minh Tien. Pham Dong Bang, Dinh Van Trung, *Using rayleigh lidar technique with large aperture newton telescope to determine atmospheric temperature distribution up to 60 km*, Advances in Applied and Engineering Physics - CAEP V, ISBN: 978-604-913-232-2(2018).

4. B. V. Hai1, D. V. Trung, P. D. Bang, T. N. Hung, N. T. T. Bao, P. M. Tien, N. T. Dien, L. T. Son, N. V. Thieu, T. V. Suu, B. H. Thai, H. V. Thanh, *Determining physical characteristics of near-field aerosol layer using lidar imaging technique*, Advances in Applied and Engineering Physics - CAEP VI, ISBN: 978-604-9985-13-3 310(2020).

5. Bui Van Hai, Nguyen Tuan Linh, Dinh Van Trung, Duong Tien Tho, Pham Dong Bang, Tran Ngoc Hung, Nguyen Thi Thanh Bao, Pham Minh Tien, *Determining the superposition function of lidar system by experimental method*, Advances in Optics, Photonics, Spectroscopy & Applications XI, ISBN: 978-604-9988-20-2(2021).

6. Bui Van Hai, Nguyen Tuan Linh, Dinh Van Trung, Duong Tien Tho, Pham Dong Bang, Tran Ngoc Hung, Nguyen Thi Thanh Bao, Pham Minh Tien, *Development of a method for measuring the surface of large-aperture aspherical mirrors by reflection imaging*, Advances in Optics, Photonics, Spectroscopy & Applications XI, ISBN: 978-604-9988-20-2 (2021).